



## Assessment on Tracking Performance of PID, Cascade Proportional Adaptive Interaction Algorithm and Nonlinear Adaptive Interaction Algorithm Controller of XY Table Ball Screw Driven System

Zain Retas<sup>1</sup>, Lokman Abdullah<sup>1,\*</sup>, Zamberi Jamaludin<sup>1</sup>, Muhamad Syafiq Syed Muhammad<sup>1</sup>, Mohd Nazmin Maslan<sup>1</sup>, Ruzaidi Zamri<sup>1</sup>, Khairun Najmi Kamaludin<sup>1</sup>, Ahmad Idil Abdul Rahman<sup>2</sup>, Maslan Zainon<sup>3</sup>, Syed Najib Syed Salim<sup>3</sup>, Arief Suardi Nur Chairat<sup>4</sup>

<sup>1</sup> Faculty of Industrial and Manufacturing Technology and Engineering, Universiti Teknikal Malaysia Melaka, Hang Tuah Jaya, 76100 Durian Tunggal, Melaka, Malaysia

<sup>2</sup> Faculty of Electronics and Computer Technology and Engineering, Universiti Teknikal Malaysia Melaka, Hang Tuah Jaya, 76100 Durian Tunggal, Melaka, Malaysia

<sup>3</sup> Faculty of Electrical Technology and Engineering, Universiti Teknikal Malaysia Melaka, Hang Tuah Jaya, 76100 Durian Tunggal, Melaka, Malaysia

<sup>4</sup> Department of Industrial Engineering, Institut Teknologi PLN, Menara PLN, Jl. Lkr. Luar Barat, RT.1/RW.1, Duri Kosambi, Kecamatan Cengkareng, Kota Jakarta Barat, Daerah Khusus Ibukota Jakarta, Jakarta 11750, Indonesia

### ARTICLE INFO

#### Article history:

Received 20 January 2025

Received in revised form 24 February 2025

Accepted 15 July 2025

Available online 8 August 2025

#### Keywords:

PID; cascade proportional adaptive interaction algorithm (CasPAI); nonlinear adaptive interaction algorithm (NAIA); xy table ball screw

### ABSTRACT

In recent years, machine tools' central focus has been achieving precise positioning, robust monitoring, low-cost manufacturing, and adaptability to disturbances. These paradigm changes have ushered in new complications for machining tool control. Owing to this reason, a simple but adaptive, robust control is proposed. This research presents a modified advanced technique to compensate for cutting force disturbances on an XY table machine tool (plant) using the base Adaptive Interaction Algorithm (AIA). The newly developed Nonlinear-AIA (NAIA) controller is created by adding a modified nonlinear function to the base AIA controller. A mathematical model of the plant is identified using the system identification's frequency response function and based on the model, the NAIA is designed. The controller is developed and simulated using MATLAB/Simulink, and experimentally validated using an actual plant. The tracking performance of the machine tool increased with NAIA, which was compared with the classical PID and the Cascading-Proportional Interaction Algorithm (CasPAI). The results indicate that the newly suggested NAIA control strategy achieved up to 60.2% improvement over PID (for the trajectory movement frequency of 0.6 Hz, ( $f=0.6$  Hz) and 53.55% improvement over at  $f=0.2$  Hz. In addition, results showed that the NAIA improves 86.29% of the root mean square error (RMSE) for  $f=0.6$  Hz over PID and 78.68% improvement over CasPAI.

\* Corresponding author

E-mail address: [lokman@utem.edu.my](mailto:lokman@utem.edu.my)

<https://doi.org/10.37934/ard.141.1.7489>

## 1. Introduction

Machine tools have been widely employed in a variety of industries including production processes [1,2]. The tracking performance of a machine tool's drive system is one component that influences its accuracy and precision [3]. Accurate and precise tracking and positioning are essential components of any machining operation as well as in crane application to name a few [4]. Positioning accuracy refers to the precision of point-to-point (PTP) applications, whereas tracking accuracy refers to the system's ability to follow a certain trajectory [5,6]. Both components have a significant impact on the results, and improving these two components will result in a higher-quality end product that will satisfy customers.

The XY table is the basic structure of a computer numerical control (CNC) machine that provides the platform for the movement of the workpiece or tool in the X and Y directions [7]. The XY table provides precision-controlled automated movement, which is commonly required for industrial procedures such as drilling, milling and many more. Positioning system tracking accuracy is gaining popularity as the demand for error minimization in the machining and assembly sectors [8].

The tracking performance of a machine tool's drive system is one component that influences its accuracy and precision. Good tracking and positioning precision in machine tool controller design approaches are among the performance characteristics that are constantly studied. Several elements, including the plant's mechanical structure, might contribute to poor system tracking performance.

Various advanced control algorithms, such as PID, CasPAi and NAIA controllers, have been evaluated for high tracking accuracy and precision [9,10]. These controllers aim to ensure stable dynamic responses with minimal overshoot and oscillations, with a focus on adaptive capabilities to handle load and friction variations [11]. The studies also discuss the computational complexity and practical implementation of these controllers, highlighting the importance of efficient and effective control strategies in achieving precise positioning in XY table systems [12].

The most critical feature of a driving system is to track performance measurements. Mechanical structure, mass variations and disturbance forces all have an impact on performance [13-15]. Friction and cutting forces are the two most common kinds of disturbance forces in machine tools. These are the most well-known disruptions that may influence the tracking performance of a machine tool [16,17].

As a result, the disturbance force generated during the cutting operation will impair the machine tool systems' position and tracking accuracy. The presence of high-frequency components causes needless extra vibration and reactivity. This may result in poor precision and influence the surface finish quality. Furthermore, mass variations may impair system performance. In certain circumstances, the mass is just a small piece of the worktable and is frequently ignored [18]. One of the methods to overcome the above problems is adaptive control. Practically, this type of controller is used to adapt to the changes occurring in the system. It provides automatic tuning to the controller parameters that make the controller more flexible [19,20]. Fu *et al.*, [21] claimed that the proposed techniques perform better than the conventional PID controller. Besides that, a new modified nonlinear function is added to the fundamental Adaptive Interaction Algorithm (AIA), resulting in a new design known as the NAIA controller, which can correct for cutting force disruption [22]. This compensatory approach is extremely practical and straightforward to apply to machine tool technology. The NAIA algorithm aims to explore unknown environments in a sample-efficient manner by maximizing the information of the next step. In this work, a new technique and contribution to compensating cutting force disturbances using the NAIA is proposed. Then, the simulation and experimental result for the controllers PID, CasPAi and NAIA is compared.

## 2. Methodology

### 2.1 Experimental Setup

For the XY Table Ball-Screw drive system by Googol Tech is utilized in the experimental work. The plant is shown in Figure 1(a). The XY milling table contains three axes: X, Y and Z. These axes are driven by three Panasonic MSMD 022G1U A.C servo motors. Only the X axis is considered to define the structure and process of designing the controller in this study. The Y and Z-axis are not considered because it is beyond the scope of the research. The components of the XY table are depicted in Figure 1(b).

The x-axis is determined as the horizontal movement. The characteristics of XY milling table are, firstly, the dimension is 630 mm (length) x 470 mm (width) x 815 mm (height), the mass of the X axis is 36.8 kg and the maximum effective travel distance of the table is 300 mm. On the other hand, for positioning measurement, both the X and Y axes are furnished with an incremental encoder. In the other hand, the sliding rod mechanism are guided and assisted by the motor and ball screw. It also shows that the three limit switches are installed in the vicinity of the three axes for safety concerns. This is to inhibit collisions at the end of the table's movement path.

The configuration of the system that consists of the personal computer (PC) is installed with MATLAB / Simulink and Control Desk for man-machine interfacing (MMI). The MMI provides the platform to insert inputs and observe and capture the real-time outputs for both numerical and experimental data via the graphical user interface (GUI). Besides the actuating plant that used the XY milling table, the data acquisition box (DAQ) used is dSPACE DS 1104 Digital Signal Processing (DSP) in this system. Then, the amplifier is used to amplify or reduce the signal from the PC to the drive system or drive system to the PC accordingly.

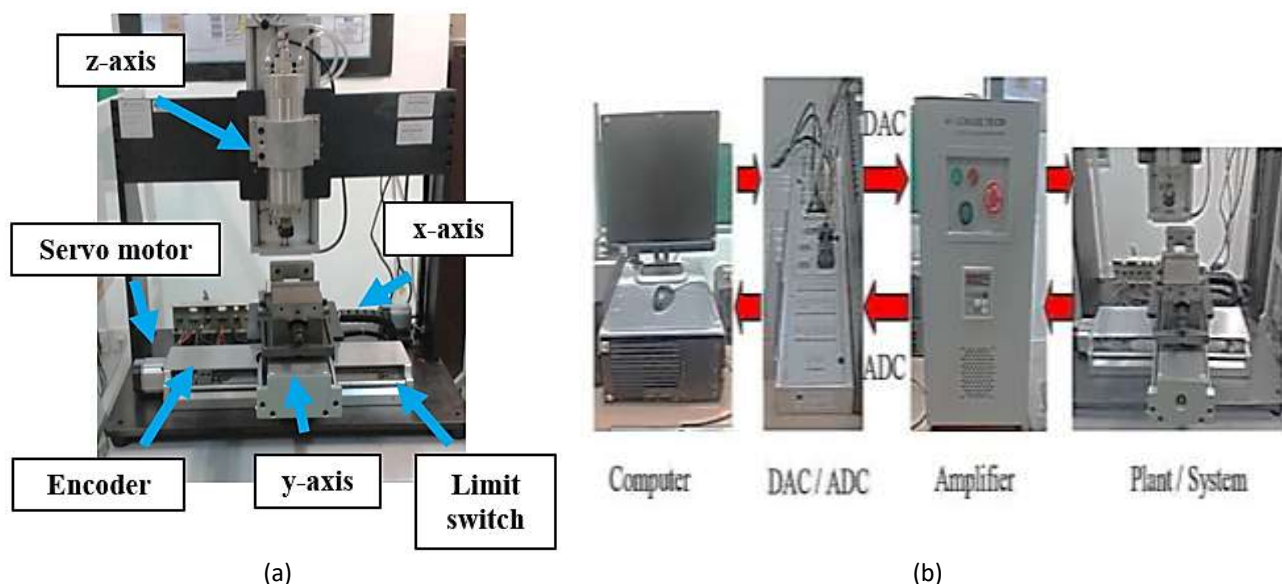


Fig. 1. (a) XY milling table, (b) The basic configuration of the experimental setup

## 3. Controller Design

### 3.1 Experimental Setup

AIA is integrated within PID controllers by constructing on theoretical interaction concept. This theory develops a more practical and pragmatic approach to achieve gradient descent in consideration space [23]. The tuning algorithm is relatively simple since it does not require complex

tuning processes. The parameters are tuned in such a way to produce minimum position error of the system. The algorithm is also generally appropriate to linear and nonlinear devices due to its simplicity.

The controller is designed based on the advanced concept of adaptive interaction. By using this principle, the control system is divided into four subsystems, which include plants, proportional, integral, and derivative controls. PID control parameters, proportional gain,  $K_p$ , integral gain,  $K_i$  and derivative gain,  $K_d$  are related to these four subsystems. The AIA controller is developed through adaptive interaction concept in which the tuned parameters of  $K_p$ ,  $K_i$  and  $K_d$  are needed.

### 3.2 Nonlinear Adaptive Interaction Algorithm (NAIA)

NAIA controller is an extension of the AIA where a nonlinear gain function is added in series with AIA controller. Figure 2 describes the control configuration of a NAIA controller and it follows with the configuration of the nonlinear function. It is known as NPID controller, is recognized by a sector bounded with nonlinear gain,  $K_e$ , that the PID controller is in series with. The self-tuned gain modification,  $K_e$  behaves as a nonlinear function bounded by  $0 < K_e < K(e_{max})$  with position tracking error,  $e_p(t)$  as shown in Eqs. (1) and (2).  $KO$  is the difference of the nonlinear gain, and  $e_{max}$  is the highest error value. The output of this nonlinear function is identified as scaled error,  $l_e$  and is defined in Eqs. (3) and (4). Eq. (5) shows the general equation of the NAIA controller [24]. On the other hand, the open loop transfer function is formed by combining Eqs. (4) and (5) as shown in Eq. (6).

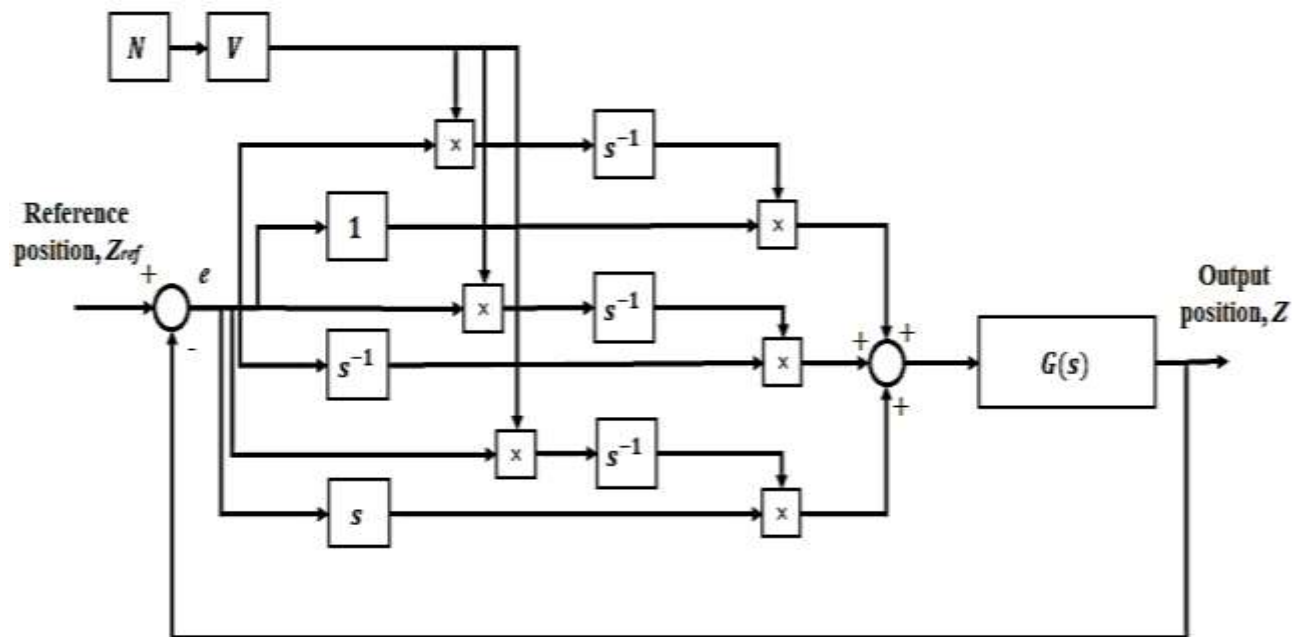


**Fig. 2.** Control structure of a nonlinear AIA (NAIA)

$$\text{Nonlinear gain, } K_e = 2 - \left( \frac{\exp(KO.e) + \exp(-KO.e)}{2} \right) \quad (1)$$

$$\text{Error, } e_{max} = \begin{cases} e & |e| \leq e_{max} \\ e_{max} \text{sign}(e) & |e| \geq e_{max} \end{cases} \quad (2)$$

$$\text{Scaled error, } l_e = K_e K_n n = 1, 2, 3 \quad (3)$$

$$K(e_{max}) = \frac{1}{[G_{openloop}(j\omega)]} \quad (4)$$

$$\text{NAIA transfer function, } G_{NAIA} = K_e K_{n1} \left[ (K_{p1}e)^2 \frac{el}{s} \right] + K_e K_2 \left[ (K_{il}e)^2 \frac{el}{s^3} \right] + K_e K_3 \left[ (K_{dl}e)^2 \frac{el}{s} \right] \quad (5)$$

Where,

function fe = fcn (e)

KO=0.4

emax=1.8;

if abs (e) <=emax,

e =e;

else

e=(max|\*sign(e);

end

Ke = 2-((exp|exp(|-KO)\*e)|)/2

Fe=Ke\*e

NAIA controller involves six tuning parameters, namely  $K_{pai}$ ,  $K_{iai}$ ,  $K_{dai}$ ,  $K_O$ ,  $e_{max}$  and  $K_p$ . The step-by-step procedure to acquire these parameters is illustrated in Figure 3. Three parameters  $K_p$ ,  $K_i$  and  $K_d$  come from the AIA control transfer function and the remaining two parameters ( $K_O$  and  $e_{max}$ ) are from the nonlinear function,  $N$ . The first step is to design the AIA controller. On the side note, the method to adjust the AIA controller parameters. The second step involves tuning of  $K_O$  and  $e_{max}$ . Recall that  $K_O$  is the amount of difference for the nonlinear gain while  $e_{max}$  is the maximum value of error.  $K_O$  and  $e_{max}$  are regulated using a heuristic (trial and error) method based on Popov's stability criterion. Procedures for the application of the Popov Stability Criterion were discussed [25]. Firstly, the maximum value of  $K_e$  is set, where the value of  $K_O$  and  $e_{max}$  is limited. The  $G_{openloop}(j\omega)$  in Eq. (7) is the real part of the intercepting point in Popov plot. The imaginary component of Eq. (8) needs to be multiplied with  $\omega$  for Popov plot.

The real and imaginary apparatuses of the transfer function are derived as:

$$G_{openloop} = \frac{A(K_d s^2 + K K_p s + K_i)}{s(s^2 + B s + C)} \quad (6)$$

$$\text{Re}G_{openloop}(j\omega) = \frac{A[(BK_d K_p)\omega^2 + CK_p - BK_i]}{B^2 \omega^2 + (C - \omega^2)^2} \quad (7)$$

$$\omega \cdot \text{Im}G_{openloop} = \frac{A[(K_d \omega^4 + (B K_p - CK_d - K_i) + K_i)\omega^2 + CK_i]}{B^2 \omega^2 + (C - \omega^2)^2} \quad (8)$$

Where,  $A = 2\zeta\omega_n$ ,  $B = \omega_n^2$  and  $C = \omega_n^2 k$ ., Symbol of zeta,  $\zeta$  = damping ratio,  $\omega_n$  = natural frequency and  $k$  = open loop gain of the system.

The value of  $\omega$  is equivalent to 16.3711. The value is obtained based on the stability region of the system. Similar gain values for linear NAIA controller as tabulated in Table 1. A Popov line indicates the tangent which is added onto the graph. Thus, the tangential line intercepted with the existing graph at point  $(-\text{Re}, j0)$ .

The crossing point is identified at  $(-0.2603, 0)$  for the x-axis. The maximum value of  $K_e$ , or  $K(e_{max})$  is calculated by applying Eq. (4). The  $K(e_{max})$  is determined as 3.8387. Meanwhile,  $K$  and  $e_{max}$  are 0.4 and 1.8mm respectively. The value is tuned based on the fact to obtain minimum possible error as well as preserving the stability region of the system.

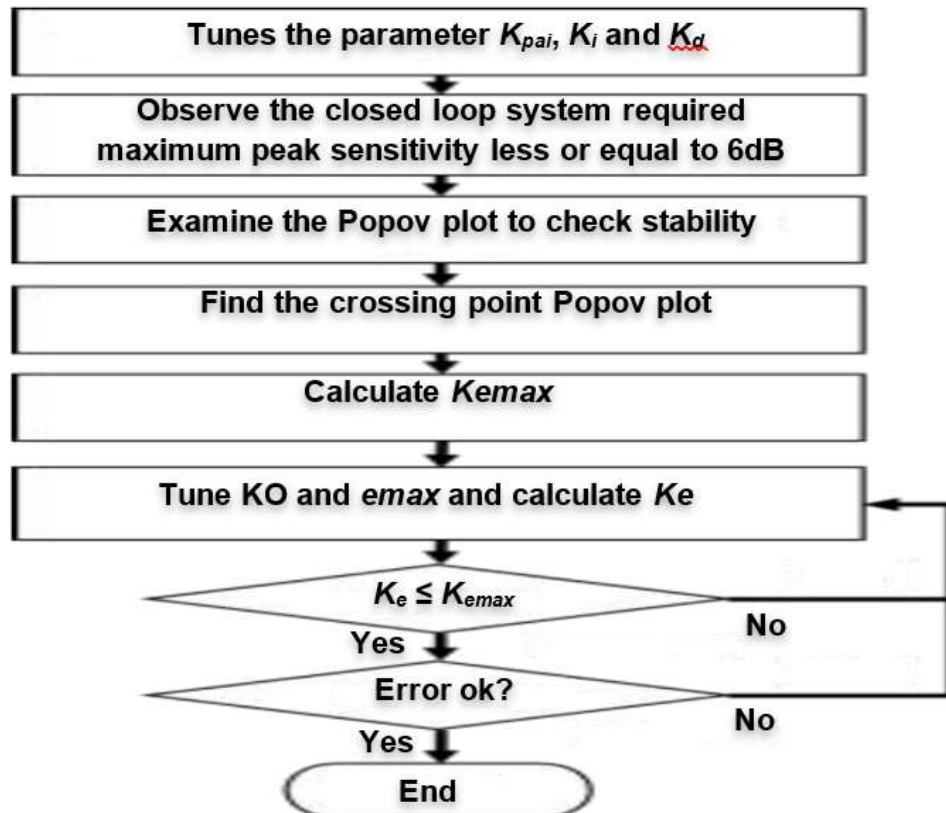


**Fig. 3.** Flowchart of the procedure to obtain parameter of NAIA controller

Generally, the value of  $e_{max}$  is selected first, followed by the value of  $KO$  [26]. The selection of  $KO$  and  $e_{max}$  are opted based on highest allowable value of nonlinear gain,  $K_e$  which depends on the range of stability. In addition, these parameters are chosen to obtain the minimum of Maximum Tracking Error. In the case of the fixed gain value of an NAIA controller, the Nyquist plot could be used for stability analysis. The non-linear gain, the  $K_e$  continues to change the NAIA controller thus causing the Nyquist plot to be no longer valid. Therefore, Popov stability criterion or Lyapunov stability criterion should be employed for the purpose. Theoretically, a system is stable if the Popov plot,  $P$  duplicates to the right of the tangential mark as shown in Figure 4(a).

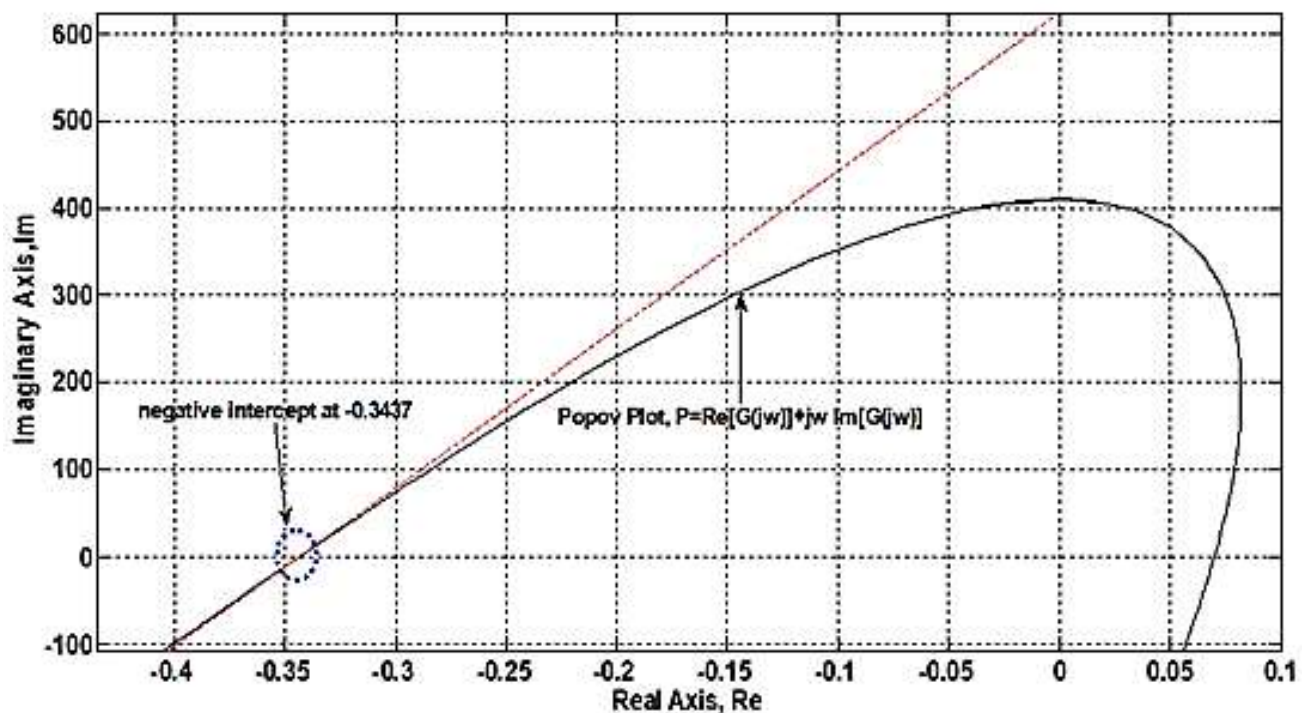
Here, the system is stable because the relevant conditions are satisfied. Figure 4(b) shows the relationship between nonlinear gains with different errors,  $e$ . The figure clearly indicates that  $K_e$  is multiplying the error. As the error value increases, the value of the nonlinear gain increases exponentially in  $K_e$ . In addition, the controller behaves like a normal PID controller when the nonlinear error equals one ( $K_e=1$ ). This means that the nonlinear function works according to the error values.

**Table 1**

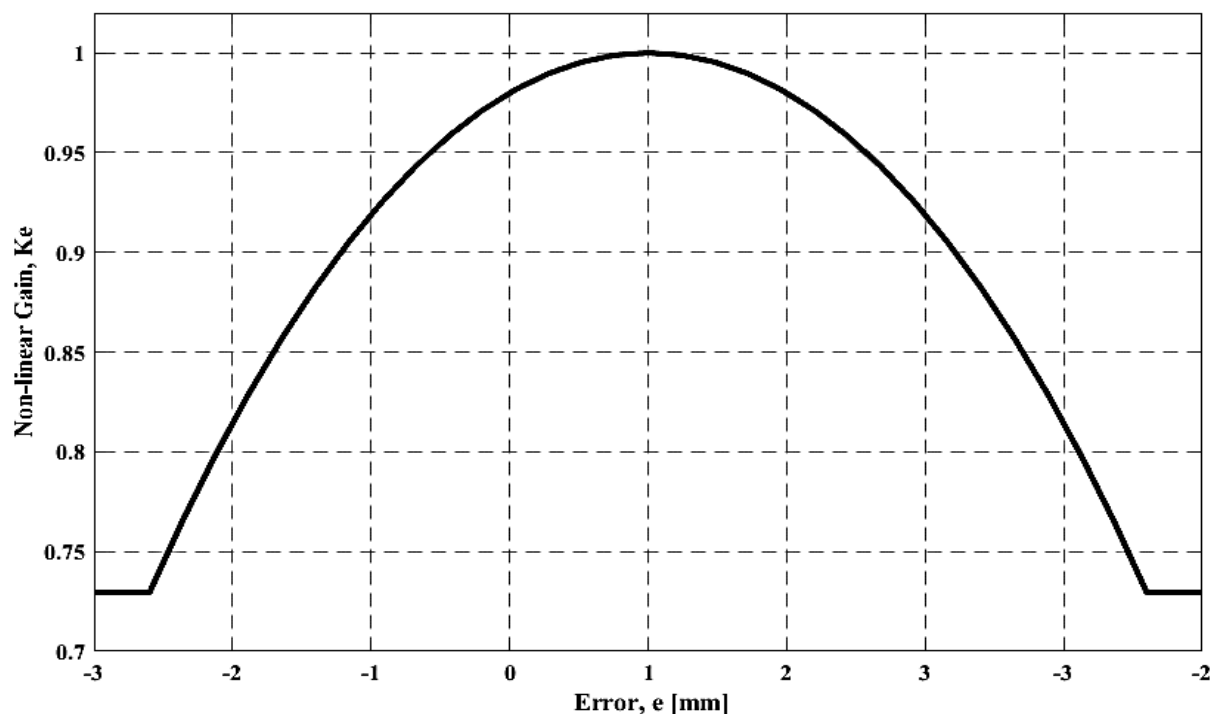
Value of tuned NAIA parameter,  $KO$  and  $e_{max}$

$K(e_{max})$	$KO$	$e_{max}$
3.8387	0.4	1.8 mm





(a) Graph Popov Plot of NPID Control



(b) Graph of Nonlinear Gain,  $K_e$  vs. Error,  $e$

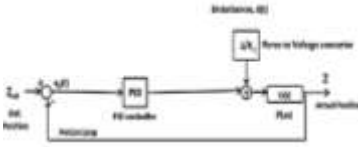
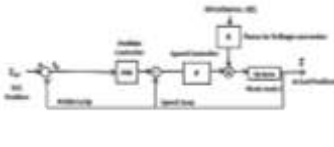
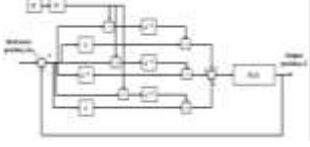
**Fig. 4.** (a) Popov plot of the NPID controlled system. (Rahmat, 2012), (b) Graph of nonlinear gain,  $K_e$  against error,  $e$

Referring to Table 2, the PID controller is a linear controller widely used in industry due to its simple structure and high practicality for implementation. It consists of proportional gain,  $K_p$ , integral gain,  $K_i$  and derivative gain,  $K_d$ , which is illustrated in Table 2. However, since it is not an adaptive

controller, it cannot compensate for different disturbances. On the other hand, a CasPAI controller is a linear controller developed by combining two modules, namely a proportional P controller with an AIA. Last, a Nonlinear AIA controller is an adaptive controller that can compensate for different disturbances. As a result, the NAIA controller outperformed the other two controllers due to its superior features in compensating for different types of disturbances.

**Table 2**

Key features of the controllers in comparison

	PID	CasPAI	NAIA
Schematic diagram			
Features	<ul style="list-style-type: none"> <li>• Consists of <math>K_P</math>, <math>K_I</math>, and <math>K_D</math> value</li> <li>• Simple and easy to tune</li> <li>• Linear controller</li> <li>• Not adaptive (does not manage to cater to different disturbances)</li> </ul>	<ul style="list-style-type: none"> <li>• Combination of cascade-P with AIA controller</li> <li>• Ability to individually tune the velocity and position loop.</li> <li>• Linear controller</li> </ul>	<ul style="list-style-type: none"> <li>• Nonlinear</li> <li>• Comparatively easy to tune than CasPAI</li> <li>• Adaptive controller (ability to cater to different disturbances)</li> </ul>
RMSE (at 2500 rpm)	0.0553	0.0424	0.0321

## 4. Results

### 4.1 Nonlinear Adaptive Interaction Algorithm (NAIA)

The control performance of the NAIA controller is analysed *via* MATLAB/ Simulink software. The control scheme of the NAIA controller is shown in Figure 5.  $Z_{ref}$  is the input reference position in the form of a sinusoidal signal with an amplitude 15 mm. Similar to previous exercises, two tracking frequencies are selected, namely 0.2 Hz and 0.6 Hz. The same configuration setup is implemented for the case of NAIA controller for cutting force disturbance. The position tracking errors,  $e_p$  of the x-axis is recorded and presented in Figure 6, Figure 7 and Table 3.

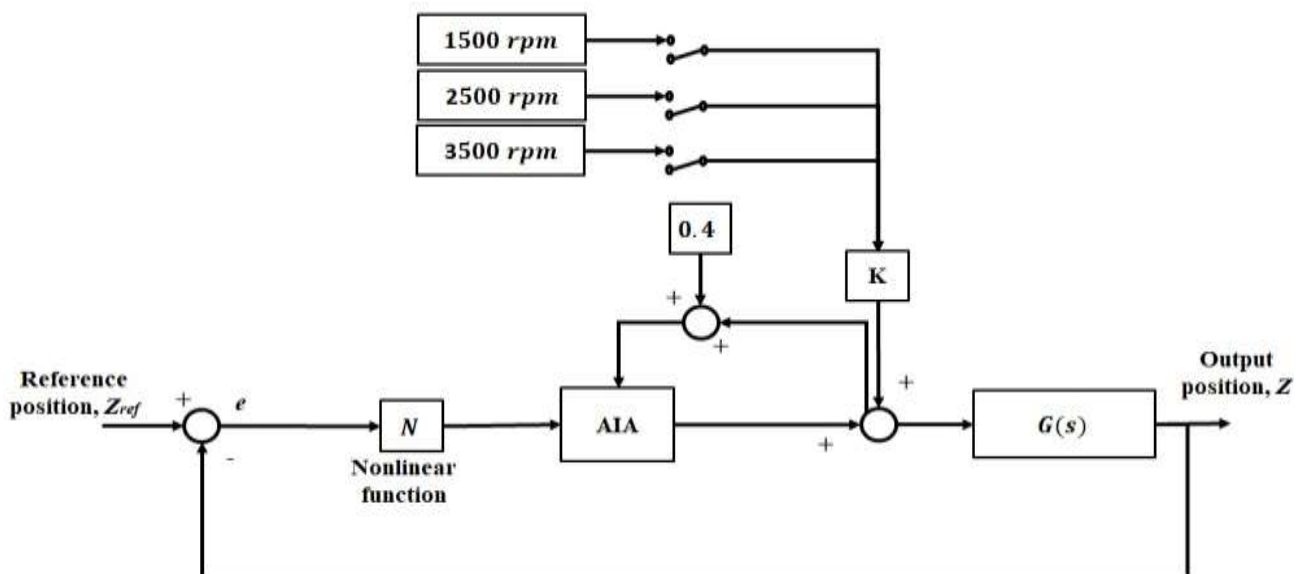


**Fig. 5.** System with NAIA controller



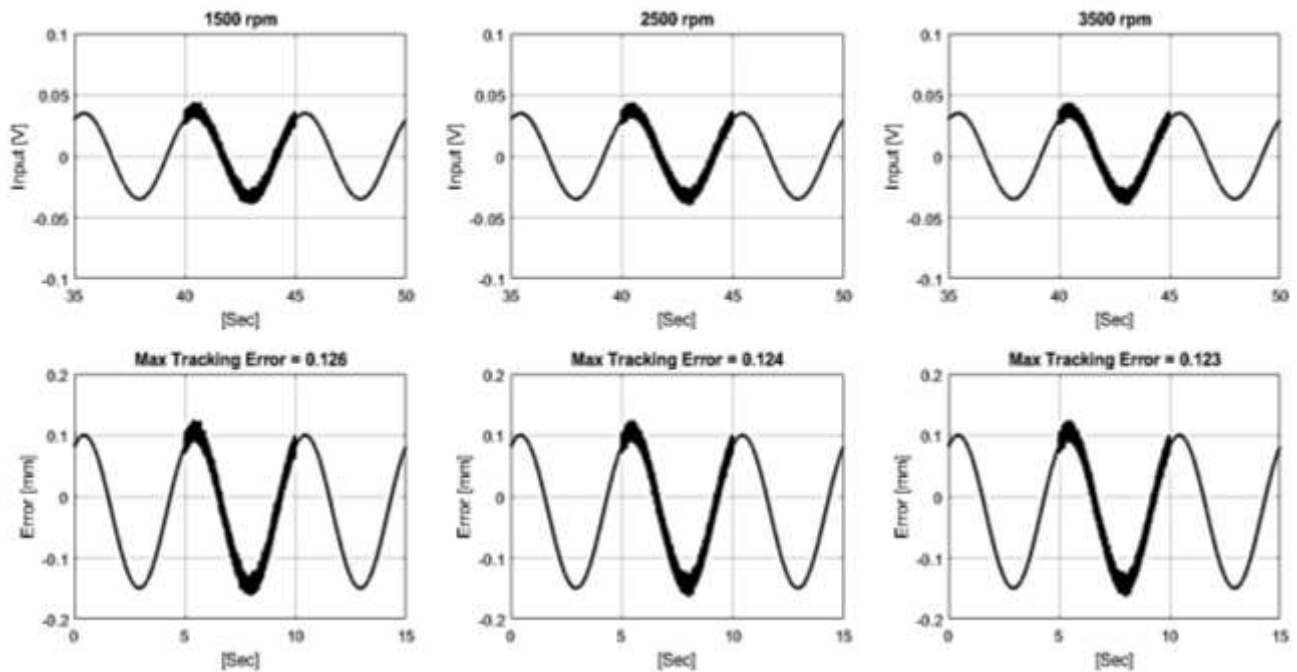


Fig. 6. Result of tracking error with NAIA controller at  $f = 0.2\text{Hz}$

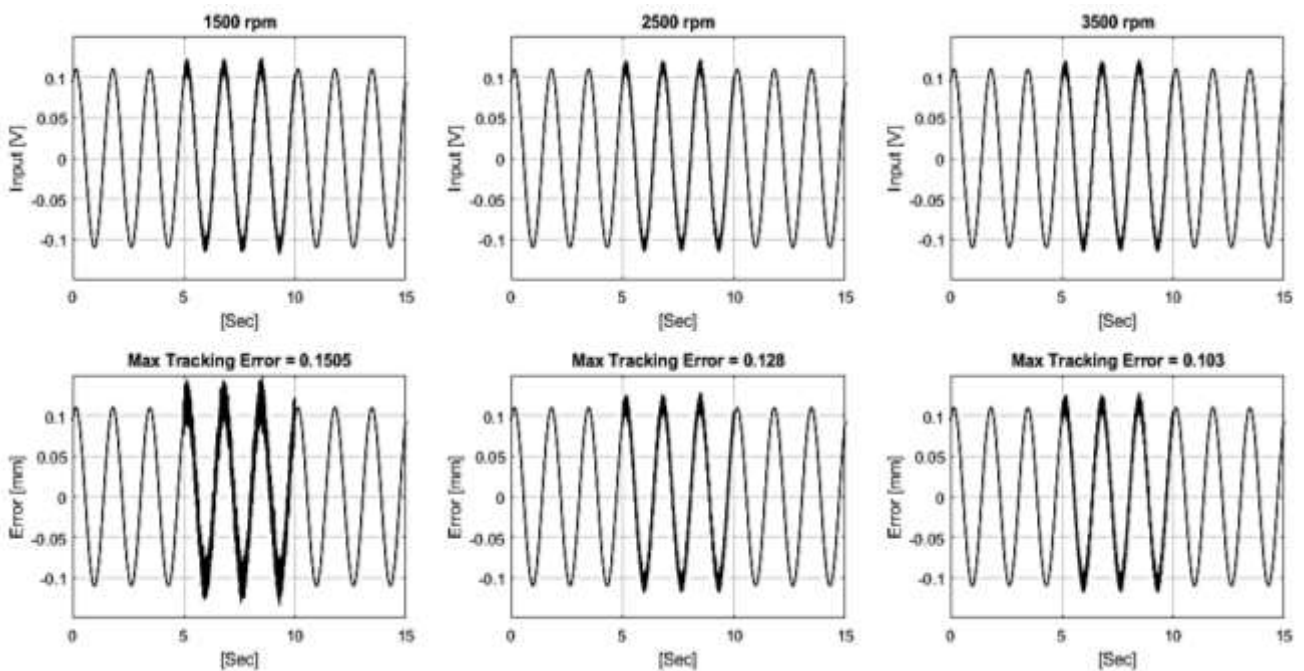


Fig. 7. Result of tracking error with NAIA controller at  $f = 0.6\text{Hz}$

**Table 3**

Maximum tracking error of system with NAIA

Spindle Speed [rpm]	Max Tracking Error [mm]		Percentage Error (%) [Track. Error / Amplitude] *100%	
	0.2 Hz	0.6 Hz	0.2 Hz	0.6 Hz
1500 rpm	0.1260	0.1505	0.8400	1.0033
2500 rpm	0.1240	0.1280	0.8267	0.8533
3500 rpm	0.1230	0.1030	0.8200	0.6867

At frequency of 0.2 Hz, the maximum tracking error of the NAIA controller produces values of 0.1230 mm (at 3500 rpm), 0.1240 mm (at 2500 rpm) and 0.1260 mm (at 1500 rpm). In terms of percentage errors, the values are converted as 0.8200% (at 3500 rpm), 0.8267% (at 2500 rpm) and 0.84% (at 1500 rpm), respectively. Meanwhile, at frequency of 0.6 Hz, the maximum tracking error is 0.1030 mm (at 3500 rpm), 0.1280 mm (at 2500 rpm) and 0.1505 mm (at 1500 rpm) with percentage errors of 0.6867% (at 3500 rpm), 0.8533% (at 2500 rpm) and 1.0033% (at 1500 rpm) respectively.

Based on observation, it is found that the faster the spindle speed rpm is, the lower the maximum tracking errors that were produced. This shows that NAIA controller is more predictable from the previous controller which is PID and CasPAi. In addition, it is also observed that the error at higher frequency (0.6 Hz) compared to at 0.2 Hz (for the case of spindle speed = 3500 rpm is lower which is oppose trend to the previous result. The reason is due to the nonlinear behaviour of the disturbance cutting force itself.

#### 4.2 Experimental Results

The PID controller was analysed using the experimental setup as shown in Figure 8. The percentage error is applied to the experimental analysis as per simulation. The highest percentage of error occurred at spindle speed of 1500 rpm which was 1.533% and 0.6366% for  $f = 0.6$  Hz and  $f = 0.2$  Hz respectively. The highest percentage error recorded for PID controller was 1.533%. The reason on why the error is maximum at 1500 rpm is due to the fact that at the spindle speed of 1500rpm, the contact point between the cutting tool with the workpiece is greater compared to at 2500rpm and 3500 rpm, thus this condition will lead to generate more errors due to the factor of larger disturbance force acted at the point of contact [27].

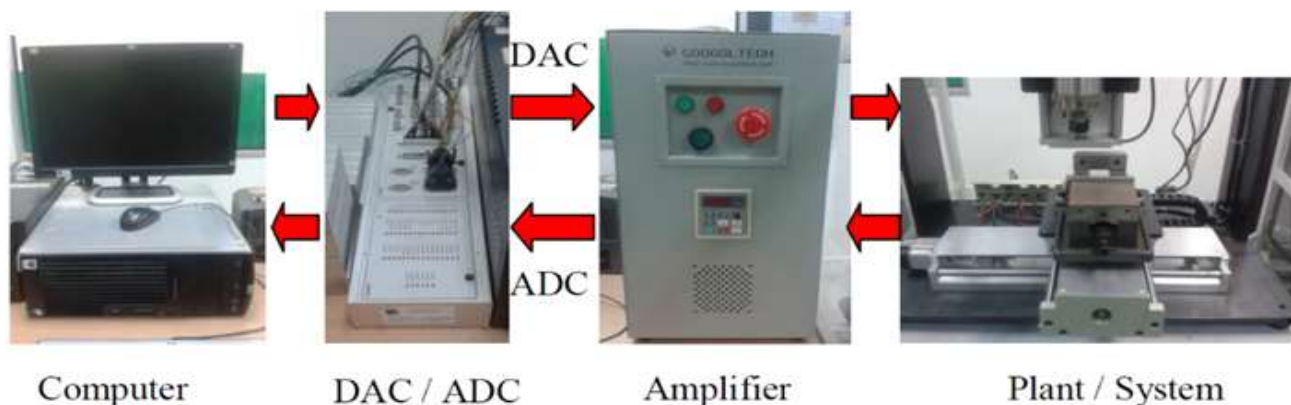


**Fig. 8.** Flow diagram of the experimental setup

#### 4.3 Corresponding Trend of Tracking Error between Controllers

Table 4 shows the percentage error reduction between controller PID, CasPAi, and NAIA. It can be concluded that the minimum improvement achieved by NAIA is 20.71% (NAIA with PID, spindle speed = 1500 rpm,  $f = 0.2$  Hz), and the maximum improvement achieved by NAIA is 60.20% (NAIA with PID, spindle speed = 3500 rpm,  $f = 0.6$  Hz). The detailed results are, for the case of (spindle speed=1500 rpm,  $f = 0.2$  Hz), it is observed that the percentage error reduction between CasPAi and PID is equivalent to -16.16%, while NAIA to PID is 20.10%. NAIA compared to CasPAi is equivalent to 31.74%. For the case of (spindle speed=1500 rpm,  $f = 0.6$  Hz), the percentage error reduction between CasPAi and PID is equivalent to 23.08%, while NAIA to PID is 40.63%. NAIA compared to CasPAi is

equivalent to 22.82%. Next, for the configuration of (spindle speed=2500 rpm,  $f = 0.2$  Hz), it is recorded that the percentage error reduction between CasPAi and PID is equivalent to -64.15%, whereas NAIA to PID is 23.76%. NAIA compared to CasPAi is equivalent to 53.55%. For the case of (spindle speed=2500 rpm,  $f = 0.6$  Hz), the percentage error reduction between CasPAi and PID is equivalent to 23.54%, while NAIA to PID is 51.96%. NAIA compared to CasPAi is equivalent to 37.17%. Meanwhile, for the setup of (spindle speed=3500 rpm,  $f = 0.2$  Hz), it is examined that the percentage error reduction between CasPAi and PID equals -12.09%, whereas NAIA with PID is 24.73%. NAIA compared with CasPAi equals to 32.84%. For the setup of (spindle speed=3500 rpm,  $f = 0.6$  Hz), the percentage error reduction between CasPAi and PID equals to 24.95%, while NAIA with PID is 60.20%. NAIA compared with CasPAi is equivalent to 46.97%. Figure 9 shows the percentage error reduction in a graphical form.

**Table 4**

Percentage of simulation error reduction between controllers

Frequency	Amplitude of Tracking Error (mm)			Error Reduction (%)		
	PID	CasPAi	NAIA	$\left[ \frac{\text{controller 1} - \text{controller 2}}{\text{controller 1}} \times 100\% \right]$		
				CasPAi with PID	NAIA with PID	NAIA with CasPAi
Spindle Speed (1500 rpm)						
0.2 Hz	0.099	0.115	0.0785	-16.16	20.71	31.74
0.6 Hz	0.2535	0.195	0.1505	23.08	40.63	22.82
Spindle Speed (2500 rpm)						
0.2 Hz	0.0926	0.1520	0.0706	-64.15	23.76	53.55
0.6 Hz	0.2498	0.191	0.1200	23.54	51.96	37.17
Spindle Speed (3500 rpm)						
0.2 Hz	0.091	0.102	0.0685	-12.09	24.73	32.84
0.6 Hz	0.2465	0.185	0.0981	24.95	60.20	46.97

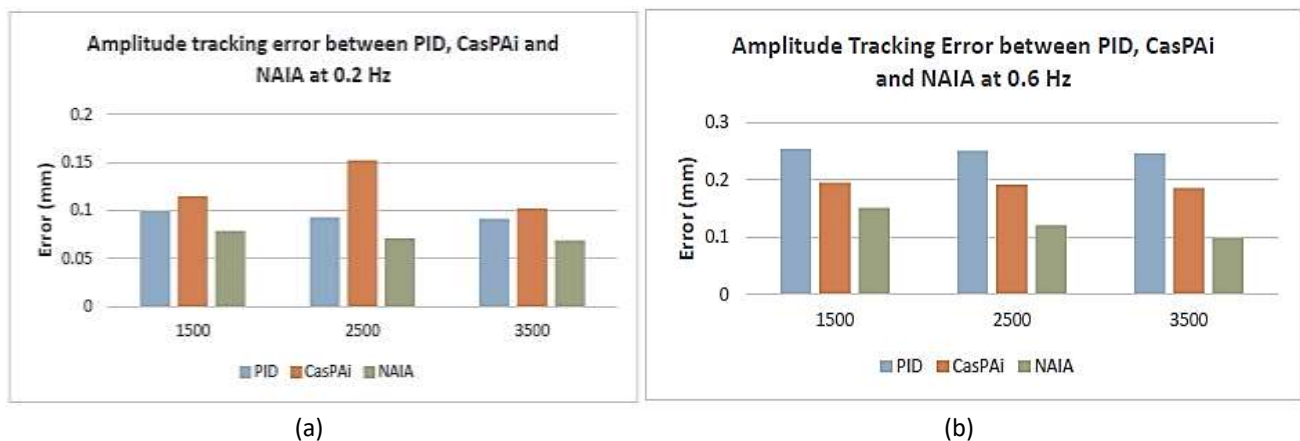


**Fig. 9.** Simulation result performance analysis based on frequency at spindle speed:(a) 0.2 Hz (b) 0.6 Hz

#### 4.4 Corresponding Trend of RMSE between Controllers

The definition of Root Mean Square Error (RMSE) is the square root of the average of the square of all errors. It is also commonly identified as the quadratic mean, which is a measurement of the magnitude difference between the current and desired point at various parameters. This method is applied in practice to solve a problem for a sinusoidal based input signal [28,29]. RMSE provides a more accurate representation of the controller tracking performance compared to normal maximum tracking error. The RMSE value will change iteratively until a point of difference is achieved at each

and every point in the tracking error. The function presented in Eq. (9) is the RMSE applied in MATLAB. The RMSE unit is in millimetre (mm). Table 5 and Figure 10 summarises the RMSE values of the measured tracking errors for the x-axis at 0.2 Hz.

$$RMSE = \sqrt{(\text{mean\_Error})^2} \quad (9)$$

**Table 5**

RMSE comparison of PID, CasPAi and NAIA at  $f = 0.2$  Hz

Spindle Speed [rpm]	Root Mean Square Error (mm)			Error Reduction (%)		
	PID	CasPAi	NAIA	CasPAi with PID	NAIA with PID	NAIA with CasPAi
1500 rpm	0.0553	0.0518	0.0415	6.33	24.95	19.88
2500 rpm	0.0553	0.0424	0.0321	23.33	24.29	41.95
3500 rpm	0.0551	0.0427	0.0324	22.50	41.20	24.12

Table 6 indicates, in all three spindle speeds at  $f = 0.2$  Hz, NAIA controller produces the least RMSE. Figure 10 shows the RMSE performance based on the data tabulated. It is observed that for PID controller, the RMSE does not change much throughout the three-spindle speed. CasPAi observes a slight reduction in RMSE when the spindle speed increases. For NAIA, the RMSE results also shows the trend of reduction when the spindle speed is increased.

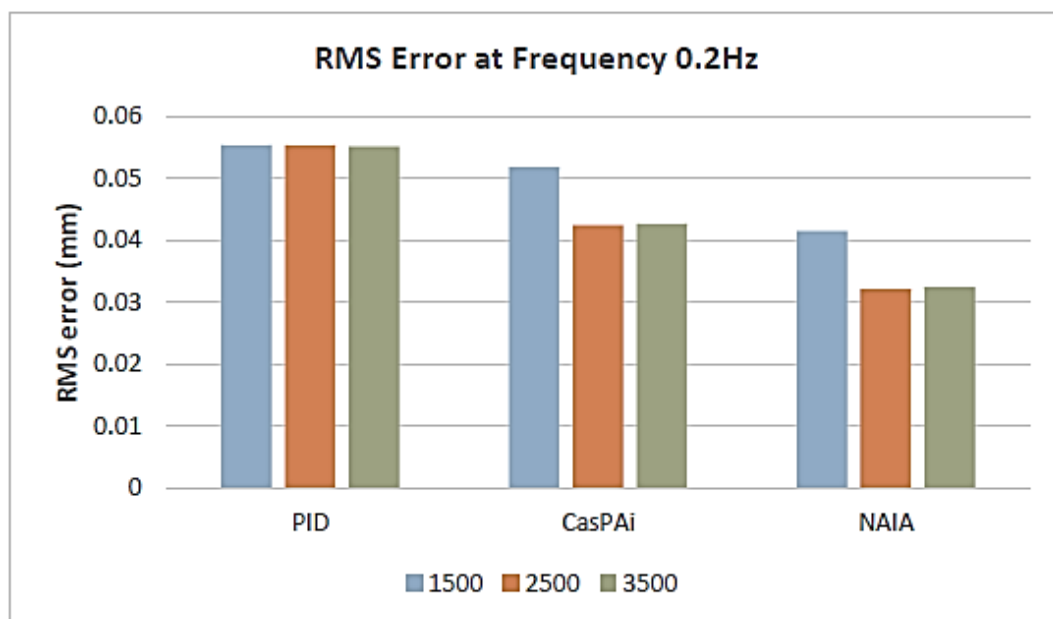


**Fig. 10.** RMSE values for different controllers and cutting forces at  $f = 0.2$  Hz

The results showed that at 0.2 Hz, NAIA controller generated the least RMSE values when subjected to the three different cutting forces. The highest RMSE value was recorded for the PID controller, as expected. This value was recorded at cutting forces measured at 1500 rpm. The research by Chiew *et al.*, [30] particularly highlights performance differences at varying RPMs, including 1500 rpm, and supports the conclusion that NAIA achieves lower RMSE values. Table 5 also contains data on percentage error reduction. The formula is stated in the following Eq. (10).

$$\text{Error Reduction (\%)} = \left[ \frac{RMSE \text{ controller B} - RMSE \text{ controller A}}{RMSE \text{ controller A}} \times 100\% \right] \quad (10)$$

A percentage error reduction is the difference in error between two controllers expressed as a percentage difference in error. The percentage error reduction between CasPAi versus PID at 0.2 Hz is 6.33%, 23.33% and 22.5% for cutting forces at spindle speeds of 1500 rpm, 2500 rpm and 3500 rpm respectively. Next, the percentage error reduction between NAIA and PID were 24.95%, 41.95% and 41.2% for cutting forces at spindle speeds of 1500 rpm, 2500 rpm and 3500 rpm respectively. Finally, the percentage error reduction between NAIA and CasPAi were 19.88%, 24.29% and 24.12% respectively. Table 6 and Figure 11 summarizes the RMSE values of measured tracking errors for the x-axis at 0.6 Hz.

**Table 6**

X-axis RMSE values for different controllers and cutting forces at  $f = 0.6$  Hz

Frequency	Root Mean Square Error (mm)			Error Reduction (%)		
	PID	CasPAi	NAIA	CasPAi with PID	NAIA with PID	NAIA with CasPAi
1500 rpm	0.1648	0.1081	0.0941	34.41	42.90	12.95
2500 rpm	0.1648	0.0797	0.0870	47.21	47.21	9.16
3500 rpm	0.1648	0.106	0.0226	35.68	86.29	78.68

Overall, when various cutting forces were applied, the NAIA controller produced the lowest RMSE values at 0.6Hz, except at 2500 rpm, where CasPAi produces a marginally lower RMSE. On the other hand, it can be concluded that the highest RMSE value was recorded for the PID controller. The value of percentage error reduction between CasPAi and PID were 34.41%, 47.21% and 35.68% for cutting forces at spindle speed of 1500 rpm. 2500 rpm, and 3500 rpm respectively. Meanwhile, the value of percentage error reduction between NAIA and PID were 42.90%, 47.21% and 86.29% for cutting forces at spindle speed of 1500 rpm. 2500 rpm, and 3500 rpm respectively. Finally, the value percentage error reduction between NAIA and CasPAi were 12.95%, 9.16% and 78.68% for cutting forces at spindle speed of 1500 rpm. 2500 rpm, and 3500 rpm respectively.

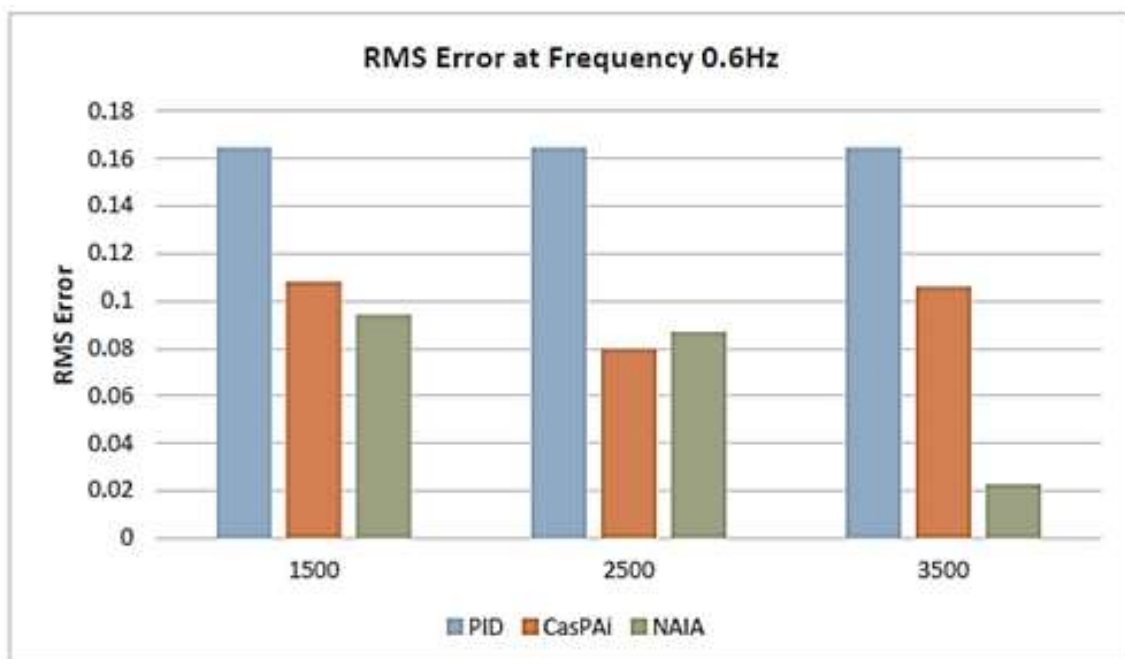


**Fig. 11.** RMSE values for different controllers and cutting force at  $f = 0.6$  Hz

#### 4.5 Corresponding Trend of Tracking Error at Different Spindle Speed

Next, it goes to corresponding trend of tracking error at different Spindle speed. Table 7 and Figure 12 shows spindle speed comparison of PID, CasPAi and NAIA at  $f = 0.2$  Hz. At all frequencies of 1500 rpm, 2500 rpm and 3500 rpm, it shows that the NAIA has the lowest tracking error compared to PID and CasPAI with the value of 0.0785, 0.0706 and 0.0685, respectively.

**Table 7**

Tracking error of spindle speed comparison of PID, CasPAi and NAIA at  $f = 0.2$  Hz

Spindle Speed [rpm]	Spindle Speed		
	PID	CasPAi	NAIA
1500 rpm	0.099	0.115	0.0785
2500 rpm	0.0926	0.152	0.0706
3500 rpm	0.091	0.102	0.0685

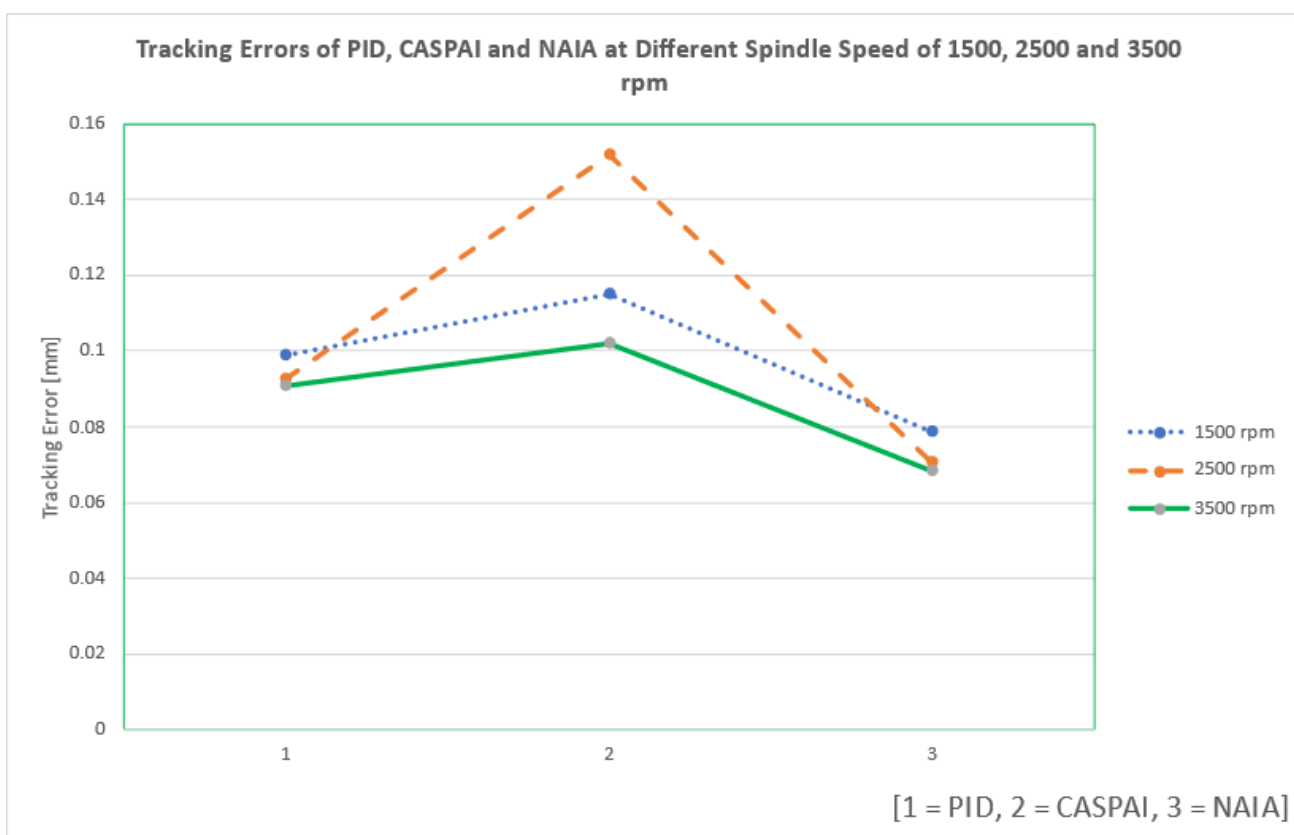


**Fig. 12.** RMSE values for different controllers and cutting force at  $f = 0.2$  Hz

## 5. Conclusions

The simulation and experimental result for the controllers PID, CasPAi, and NAIA are developed. These controllers were evaluated based on two performance measures namely maximum tracking error and RMSE. The tracking error results achieved *via* experimental work produced slightly higher maximum tracking error compared to simulation work which can be attributed from the external factors. The overall result of simulation and experimental shows that the NAIA controller produces a better tracking performance with smallest maximum tracking error. At 1500 rpm, NAIA produced the lowest RMSE values, while the highest RMSE was observed with the PID controller. The experimental results confirmed that NAIA outperformed the other controllers by providing up to 60.2%



improvement over PID and 53.55% over CasPAi in tracking accuracy. The RMSE error from NAIA is the lowest, followed by CasPAi and PID controller. It is due to the effectiveness of adaptively  $K_{\max}$  and KO of the NAIA controller structure design on tracking error, thus resulting an improvement of tracking performance of the system under the presence of cutting force disturbance.

### Acknowledgement

The authors would like to acknowledge the financial support by Ministry of Higher Education (MOHE) of Malaysia through the Fundamental Research Grant Scheme (FRGS) with reference no. FRGS/2020/TK0/UTEM/02/33 and Universiti Teknikal Malaysia Melaka (UTeM) for all the supports.

### References

- [1] Singh, Rajender. *Introduction to basic manufacturing process and workshop technology*. New Age International, 2006.
- [2] Angelopoulos, Angelos, Emmanouel T. Michailidis, Nikolaos Nomikos, Panagiotis Trakadas, Antonis Hatziefremidis, Stamatis Voliotis, and Theodore Zahariadis. "Tackling faults in the industry 4.0 era—a survey of machine-learning solutions and key aspects." *Sensors* 20, no. 1 (2019): 109. <https://doi.org/10.3390/s20010109>
- [3] Kalbasi Shirvani, Hessam. "Multivariable System Identification, Enhanced Disturbance Rejection, and Precision Motion Control for CNC Machine Tool Feed Drives." (2021).
- [4] Syazwin, Aina, Liyana Ramli, and Izzuddin M. Lazim. "A Review of Anti-Swing Control for Cranes." *Semarak Proceedings of Applied Sciences and Engineering Technology* 1, no. 1 (2025): 121-125. <https://doi.org/10.37934/spaset.1.1.121125a>
- [5] Saito, Akinori, and Yoji Jimba. "Simple Measuring of Positioning Accuracy for Machining Centers Using Image Matching." *International Journal of Automation Technology* 17, no. 5 (2023): 486-493. <https://doi.org/10.20965/ijat.2023.p0486>
- [6] Xin, Zhou, and Li Jing. "Position tracking control of an ultra-precision servo system." In *2022 International Workshop on Advanced Patterning Solutions (IWAPS)*, pp. 1-3. IEEE, 2022. <https://doi.org/10.1109/IWAPS57146.2022.9972296>
- [7] Tung, Tran Thanh, Nguyen Xuan Quynh, and Tran Vu Minh. "Development and Implementation of a Mini CNC Milling Machine." *Acta Marisiensis. Seria Technologica* 18, no. 2 (2021): 24-28. <https://doi.org/10.2478/amset-2021-0014>
- [8] Abdi, Ali. "Design and control of an XY precision positioning system using impact drive mechanism." *Recent Patents on Mechanical Engineering* 14, no. 4 (2021): 528-540. <https://doi.org/10.2174/2212797614666210129150320>
- [9] Kumar, Rajesh, and Jitendra Prasad Khatait. "Design of XY Air Bearing Stage for Ultra-Precision." In *Machines, Mechanism and Robotics: Proceedings of iNaCoMM 2019*, pp. 1087-1103. Singapore: Springer Singapore, 2021. [https://doi.org/10.1007/978-981-16-0550-5\\_104](https://doi.org/10.1007/978-981-16-0550-5_104)
- [10] Abd Latip, Siti Fadilah, and Mohd Ariffanan Mohd Basri. "Computer-Based FTC System for Flexible Robot Manipulator System under Actuator and Sensor Faults." *Semarak Proceedings of Applied Sciences and Engineering Technology* 1, no. 1 (2025): 76-83. <https://doi.org/10.37934/spaset.1.1.7683a>
- [11] Fang, Jingzhe, Tao Zhang, Xiyu Chen, Chen Qi, Guopeng Zhang, Hualiang Zhang, and Hongyu Yan. "Position Control of XY Precision Planar Motion Stage Based on Iterative Learning and Cross-coupling." In *2023 IEEE 12th Data Driven Control and Learning Systems Conference (DDCLS)*, pp. 699-704. IEEE, 2023. <https://doi.org/10.1109/DDCLS58216.2023.10165915>
- [12] Abdullah, L., Z. Jamaludin, T. H. Chiew, N. A. Rafan, and M. Y. Yuhazri. "Extensive Tracking Performance Analysis of Classical feedback control for XY Stage ballscrew drive system." *Applied Mechanics and Materials* 229 (2012): 750-755. <https://doi.org/10.4028/www.scientific.net/AMM.229-231.750>
- [13] Gayathri, N., M. Sundar, R. Sargurunathan, R. Sudharsan, and A. Sajith. "Design of Voice Controlled Multifunctional Computer Numerical Control (CNC) Machine." In *2022 International Conference on Inventive Computation Technologies (ICICT)*, pp. 657-663. IEEE, 2022. <https://doi.org/10.1109/ICICT54344.2022.9850659>
- [14] Hanifzadegan, Masih, and Ryoza Nagamune. "Tracking and structural vibration control of flexible ball-screw drives with dynamic variations." *IEEE/ASME Transactions on Mechatronics* 20, no. 1 (2014): 133-142. <https://doi.org/10.1109/TMECH.2014.2298241>
- [15] Peng, Linfa, Jianming Mai, Tianhao Jiang, Xinmin Lai, and Zhongqin Lin. "Experimental investigation of tensile properties of SS316L and fabrication of micro/mesochannel features by electrical-assisted embossing process." *Journal of Micro-and Nano-Manufacturing* 2, no. 2 (2014): 021002. <https://doi.org/10.1115/1.4026884>

- [16] Ruderman, Michael, Makoto Iwasaki, and Wen-Hua Chen. "Motion-control techniques of today and tomorrow: a review and discussion of the challenges of controlled motion." (2020). <https://10.1109/MIE.2020.2967999>
- [17] Altintas, Yusuf, Alexander Verl, Christian Brecher, Luis Uriarte, and Günther Pritschow. "Machine tool feed drives." *CIRP annals* 60, no. 2 (2011): 779-796. <https://doi.org/10.1016/j.cirp.2011.05.010>
- [18] Fan, Shi-xun, Da-peng Fan, Hua-jie Hong, and Zhi-yong Zhang. "Robust tracking control for micro machine tools with load uncertainties." *Journal of Central South University* 19, no. 1 (2012): 117-127. <https://doi.org/10.1007/s11771-012-0980-y>
- [19] Halicioglu, Recep, L. Canan Dulger, and A. Tolga Bozdana. "An automation system for data processing and motion generation." In *2017 International Artificial Intelligence and Data Processing Symposium (IDAP)*, pp. 1-9. IEEE, 2017. <https://doi.org/10.1109/IDAP.2017.8090294>
- [20] Yang, Haojin, Zihao Wang, Tao Zhang, and Fuxin Du. "A review on vibration analysis and control of machine tool feed drive systems." *The International Journal of Advanced Manufacturing Technology* 107 (2020): 503-525. <https://doi.org/10.1007/s00170-019-04702-1>
- [21] Fu, Lanhui, Lei Zhou, Jianan Liang, and Mingyong Lin. "PID parameters self-tuning based on simplex method." In *2018 Chinese Control And Decision Conference (CCDC)*, pp. 4769-4774. IEEE, 2018. <https://doi.org/10.1109/CCDC.2018.8407931>
- [22] Blanke, Matthieu, and Marc Lelarge. "Flex: an adaptive exploration algorithm for nonlinear systems." In *International Conference on Machine Learning*, pp. 2577-2591. PMLR, 2023. <https://doi.org/10.48550/arXiv.2304.13426>
- [23] Samsudin, S. I, Siti Fatimah Sulaiman, Khairuddin Osman, S. I. M. Salim, and Sazuan Nazrah Mohd Azam. 2022. "Development of Nonlinear Adaptive PI Controller For Improved Pneumatic Actuator System". *International Journal of Integrated Engineering* 14 (6): 206-15. <https://doi.org/10.30880/ijie.2022.14.06.018>
- [24] Lin, Feng, Robert D. Brandt, and George Saikalis. "Self-tuning of PID controllers by adaptive interaction." In *Proceedings of the 2000 American Control Conference. ACC (IEEE Cat. No. 00CH36334)*, vol. 5, pp. 3676-3681. IEEE, 2000. <https://doi.org/10.1109/ACC.2000.877036>
- [25] Su, Y. X., Dong Sun, and B. Y. Duan. "Design of an enhanced nonlinear PID controller." *Mechatronics* 15, no. 8 (2005): 1005-1024. <https://doi.org/10.1016/j.mechatronics.2005.03.003>
- [26] Rahmat, M. F., Sy Najib Sy Salim, N. H. Sunar, Ahmad Athif Mohd Faudzi, Zool Hilmi Ismail, and K. Huda. "Identification and non-linear control strategy for industrial pneumatic actuator." *International Journal of the Physical Sciences* 7, no. 17 (2012): 2565-2579. <https://doi.org/10.5897/IJPS12.151>
- [27] Kalpakjian, S., 2013. *Manufacturing Processes for Engineering*. Addison Wesley
- [28] Jamaludin, Zamberi, H. V. Brussel, and Jan Swevers. "Classical cascade and sliding mode control tracking performances for a xy feed table of a high-speed machine tool." *International Journal of Precision Technology* 1, no. 1 (2007): 65-74. <https://doi.org/10.1504/IJPTech.2007.015345>
- [29] Heng, Chiew Tsung, Zamberi Jamaludin, Ahmad Yusairi Bani Hashim, Lokman Abdullah, and Nur Aidawaty Rafan. "Design of super twisting algorithm for chattering suppression in machine tools." *International Journal of Control, Automation and Systems* 15, no. 3 (2017): 1259-1266. <https://doi.org/10.1007/s12555-016-0106-7>
- [30] Chiew, Tsung Heng, Weng Kang Chow, Zamberi Jamaludin, Ahmad Yusairi Bani Hashim, Lokman Abdullah, and Nur Aidawaty Rafan. "Design and analysis of modified nonlinear pid controller for disturbance suppression in machine tools." In *Symposium on Intelligent Manufacturing and Mechatronics*, pp. 105-115. Singapore: Springer Nature Singapore, 2021. [https://doi.org/10.1007/978-981-16-8954-3\\_11](https://doi.org/10.1007/978-981-16-8954-3_11)